# Mean-Adaptive Real-Coding Genetic Algorithm and its Applications to Electromagnetic Optimization (Part Two)

*Viktor OTEVŘEL, Zbyněk RAIDA*

Dept. of Radio Electronics, Brno University of Technology, Purkyňova 118, 612 00 Brno, Czech Republic

viktor.otevrel@seznam.cz, raida@feec.vutbr.cz

**Abstract.** *In the paper, a novel instance of the real-coding genetic algorithm (RCGA), called the Mean-adaptive real-coding genetic algorithm (MAD-RCGA), is applied along with other RCGAs, to selected problems in microwaves. The problems include the design of a microstrip dipole, the design of frequency-selective surfaces, and the design of a Yagi antenna. Apart from other things, the purpose of this paper is to compare these instances with MAD-RCGA on problems having some technical relevance.*

## Keywords

Mean-adaptive real-coding genetic algorithm, planar dipole, frequency-selective surface, Yagi antenna.

## 1. Introduction

The content of this paper is devoted to applications of the Mean-adaptive real-coding genetic algorithm (MAD-RCGA), being put forward in [14], along with other RCGA instances to solving complex problems in microwave technique. These RCGA instances, representing the state of the art in single-objective optimization, include:

- The minimal generational gap model (MGG) featuring the multi-parent unimodal normally distributed recombination operator (UNDX) ([4], [5], [6], [7], [8]). We will refer to this instance as MGG-UNDX.
- The generalized generational gap model (G3) featuring UNDX and the parent-centric recombination operator (PCX) ([4], [5], [6], [7], [8]). We will refer to these instances as G3-UNDX and G3-PCX.
- A two-loop RCGA with adaptive control of mutation step sizes (TRAMSS) featuring blend crossover (BLX-α) and fuzzy recombination (FR) [9]. We will refer to these instances as TRAMSS-BLX and TRAMSS-FR.
- The scaled probabilistic crowding RCGA (SPC) with parent-centric normal crossover (PNX) [1]. We will refer to this instance as SPC-PNX.
- A real-coding memetic algorithm (RCMA) with crossover hill-climbing (XHC) [11]. We will refer to this instance as RCMA-XHC.

The mission of this paper is threefold:

- To demonstrate the applicability of the algorithms to complex problems arising in electromagnetics.
- To exemplify the usage of the algorithms by their applying to a set of real-life problems.
- To compare MAD-RCGA with other RCGA instances, as regards their performances, on problems having some technical relevance.

The problems to be optimized include:

- The design of a planar (microstrip) dipole (MD).
- The design of a Yagi antenna (YA).
- The design of frequency-selective surfaces (FSSs).

Within the experiments conducted in this paper, we have derived the settings for the configuration parameters associated with MGG-UNDX, G3-PCX, G3-UNDX, RCMA-XHC, TRAMSS-BLX, TRAMSS-FR and SPC-PNX on the basis of those used and proposed in the original literature.

## 2. Setting the Experiments

Prior to starting off the experiments, we will briefly summarize the used configurations of the algorithms. For clarity, the symbols used in this section are the same as those used in the original literature.

- MGG-UNDX: It is set up on the basis of the parametric study carried out in [4], [5], [6], [7], [8] as follows:
  - The population size is fixed to 100.
  - The number of offspring is set to 6.
  - The number of parent is set to 3.
  - In UNDX, both of the used standard deviations are set for all of the problems as recommended.
  - The number of individuals selected for replacement is fixed to 2.
- G3-PCX: It is set up on the basis of the parametric study carried out in ([4], [5], [6], [7], [8]) as follows:
  - The population size is fixed to 100.
  - The number of offspring is set to 2.

- The number of parents is set to 3.
- In PCX, both of the used standard deviations are set to:
  - 0.5 when applied to the design of an MD (it is due to using discretely-changing parameters).
  - A recommended value of 0.1 when applied to the rest of the problems.
- The number of individuals selected for replacement is fixed to 2.

- G3-UNDX: It is set up on the basis of the parametric study carried out in ([4], [5], [6], [7], [8]) as follows:
  - The population size is fixed to 100.
  - The number of offspring is set to 2.
  - The number of parents is set to 3.
  - In UNDX, both of the used standard deviations are set for all of the problems as recommended.
  - The number of individuals selected for replacement is fixed to 2.
- RCMA-XHC: It is configured as used in the original paper [11].
- TRAMSS: It is configured as used in the original paper [9]. As mentioned in Section 1, we have used two TRAMSS instances differing in a choice of a recombination operator i.e., one instance takes advantage of the FR operator ([2], [10]) and the other takes advantage of the BLX-$\alpha$ operator. Moreover, we decreased the maximum number of generations, denoted as $G_0$, allowed in the inner loop from 100 to:
  - 50 when applied to the design of an MD,
  - 20 when applied to the rest of the problems.
- SPC-PNX: It is configured on the basis of the original paper [1] as follows:
  - The population size is fixed to 40.
  - The number of offspring is set to 2.
  - In PNX, the coefficient $\eta$ is set to 2.
- MAD-RCGA [14]: It is configured as follows:
  - As a parent selection mechanism, binary tournament selection (BTS) is used. All parents to which BTS is applied are sampled uniformly randomly without replacement so that there is no parent participating in BTS twice at a given generation.
  - The number of parents $\chi$ taking part in parameter-wise recombination (PWX) is set to 4.
  - The number of offspring $\lambda$ is set to:
    - 40 when applied to the design of an MD,
    - 10 when applied to the rest of the problems.
  - The population size $N_{pop}$ is set to:
    - 60 when applied to the design of an MD (i.e., the ratio $\lambda/N_{pop}$ is equal to 2/3),
    - 30 when applied to the rest of the problems (i.e., the ratio $\lambda/N_{pop}$ is equal to 1/3).
  - $max_{GMASS\text{-}CVM}$ is set to 30.
  - $max_{MAM}$ is set to 5.
  - The coefficient $\beta$ is set to 0.1.
  - The mutation rate $p_m$ is set to:
    - 0.1 when applied to the design of an MD,
    - 0 when applied to the rest of the problems (i.e., eliminating the effects of the GMASS-CVM operator).
  - The initial upper step size bound $s$ is set to 10.
  - The learning rate $\tau$ (i.e., the mutation strength on the global step size level) is set to 0.05.
  - The vector $\mathbf{m}_{step}$, keeping mutation step size values, is initialized as stated in Section 3.
  - The vector $\mathbf{f}_{reduction}$, keeping reduction factor values associated with the respective mutation step sizes, is filled up with twos.

In all the experiments, the initial population is scattered uniformly randomly over the search space. If a new solution happens to become outside a pre-defined region, it is returned back to the very point of its leaving the region i.e., the part of the solution exceeding the boundaries of the region is cut away. For each optimization problem, each algorithm is run 20 times. The maximum number of fitness function evaluations, representing a termination criterion, is fixed to:

- $2 \cdot 10^4$ for optimizing an MD,
- $2 \cdot 10^3$ for optimizing a YA,
- and $10^3$ when applied to FSSs.

The best results achieved at the end of each run are recorded. The mean and standard deviation computed from these results serve as the only performance metric used for comparison of the algorithms when applied to the design of an MD and the design of a YA. In case of applying to the design of FSSs, the performance metric is defined as the best, median and worst number of function evaluations desired for achieving a function value that is equal to or less than $10^{-1}$ (i.e., it serves as an additional termination criterion) in a maximum of $10^3$ evaluations.

# 3. The Design of a Microstrip Dipole

In this section, the instances of the aforementioned algorithms will be applied to the optimization of an MD. In order to accelerate the overall optimization process, a neural model of an MD has been developed. The neural model consists of 4 inputs and 3 outputs. The input parameters are as follows (see Fig. 1):

- The length of an MD – $A$.
- The width of an MD – $B$.
- The height of a substrate – $h$.
- The dielectric constant of a substrate – $\varepsilon_r$.

The two output parameters are represented by the real $R$ and imaginary $X$ parts of the input impedance of an MD. Training patterns were computed by means of the Method of Moments for a frequency of 30 GHz [3] under the assumption that the metallic parts of an MD are made of perfect conductors.

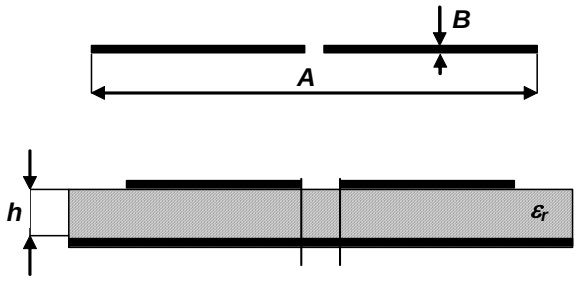


**Fig. 1.** Structure and parameters of the optimized MD.

The objective of the optimization process is to find such values of parameters $A$, $B$, $h$, $\varepsilon_r$ that are associated with an input impedance of (200 + j 0) Ω. The corresponding fitness function is defined by the following dimensionless form:

$$f_{fitness} = \sqrt{(R-200)^2 + X^2}. \qquad (1)$$

The optimization process is restricted to the following search space:

- Allowed substrate heights are $h \in \{1.0\text{ mm}, 1.5\text{ mm}\}$.
- Allowed permittivities are $\varepsilon_r \in \{1.0, 1.6, 2.0, 2.2\}$.
- Allowed dipole lengths are $A \in [10\text{ mm}; 80\text{ mm}]$.
- Allowed dipole widths are $B \in [0.01\text{ mm}; 0.50\text{ mm}]$.

In other words, $h$ and $\varepsilon_r$ represent discrete parameters, whereas $A$ and $B$ represent continuous parameters.

## 3.1 Results

Because there are two parameters, $h$ and $\varepsilon_r$, in the model taking on a finite number of non-contiguous values only, they have to be appropriately transformed in order for the model to be directly exploitable in continuous optimization. This transformation is simply accomplished as follows. Each value a given discrete parameter can take on is assigned an index from one to the maximum number of possible values the parameter can have so that after making this assignment, $h$ can take on values 1 (corresponds to 1.0 mm) and 2 (corresponds to 2.0 mm), $\varepsilon_r$ can take on values 1 (corresponds to 1.0), 2 (corresponds to 1.6), 3 (corresponds to 2.0) and 4 (corresponds to 2.2). Thereafter, the optimization process is expected to treat these two parameters as they were defined in continuous intervals of [1; 2] for $h$ and [0.5; 4.495] for $\varepsilon_r$. Prior to evaluation, the values of the parameters are rounded and transformed back to their original values by means of obtained indices. The boundaries of the intervals are chosen with respect to giving each integer value in the intervals approximately the same chance of being obtained by rounding. The above steps provide a simple way of transforming a finite set of non-contiguous values to a continuous interval, which allows the exploitation of any meta-heuristic for continuous optimization.

| EA | Fitness function values | | |
|---|---|---|---|
| | Mean | Standard deviation | Success [%] |
| MGG-UNDX | 1.4715e+001 | 8.9751e+000 | 0 |
| G3-PCX | 1.7966e+001 | 4.3188e+001 | 45 |
| G3-UNDX | 3.8811e+000 | 7.3798e+000 | 50 |
| SPC-PNX | 2.4402e+000 | 1.2946e+000 | 20 |
| RCMA-XHC | **1.2573e+000** | **1.5798e+000** | **55** |
| TRAMSS-FR | 8.2538e+000 | 5.5155e+000 | 0 |
| TRAMSS-BLX | 1.8011e+001 | 3.5661e+001 | 0 |
| MAD-RCGA | 2.8288e+000 | 9.6744e-001 | 10 |

**Tab. 1** Performance comparisons carried out on the MD model between the instances of the following algorithms: MGG-UNDX, G3-PCX, G3-UNDX, SPC-PNX, RCMA-XHC, TRAMSS-FR, TRAMSS-BLX and MAD-RCGA. "Success" in the last column refers to how many runs reached the prescribed accuracy. The best results are printed bold.

In these experiments, the vector $\mathbf{m}_{step}$, belonging to the configuration of MAD-RCGA (see Section 1), was filled with the following initial values of mutation step sizes (i.e., each per parameter):

- 3 for the parameter $A$,
- 0.02 for the parameter $B$,
- 0.5 for the parameter $h$,
- 2 for the parameter $\varepsilon_r$.

The values of the step sizes were chosen to be approximately as large as halves of their allowed ranges (i.e., transformed ranges in case of the discrete parameters). The termination criterion regarding the maximum number of function evaluation was extended by another criterion prescribing a target accuracy of $10^{-10}$ so that if any of these two criteria is satisfied, the related run will be ended.

This additional criterion is used for estimating the computational reliability of the algorithms on this model (i.e., judged with respect to all the pre-defined restraints). The results those have been obtained using all of the algorithms on the neural model of an MD are summarized in Tab. 1; the best and worst values are given in Tab. 2.

Looking into Tab.1, we can see that the best results have been achieved by RCMA-XHC. This gain in performance can be put down to the fact that apart from doing good exploration work, RCMA-XHC also performs extensive local search by means of XHC. Nonetheless, the results provided by MAD-RCGA are comparable to those

obtained by RCMA-XHC, SPC-PNX and G3-UNDX. The differences in performance between these algorithms are not so significant. Therefore, we can conclude by saying that the quality of results achieved by MAD-RCGA is able to keep in step with that obtained by the other algorithms on this optimization problem. The standard deviation values in Tab.1 along with the best and worst values summarized in Tab. 2 also show that the spread of fitness function values obtained by MAD-RCGA, RCMA-XHC and SPC-PNX over all their runs is the least when compared to the other algorithms. A comparison of typical convergence behavior of the used algorithms made for their best-performing runs is depicted in Fig. 2.

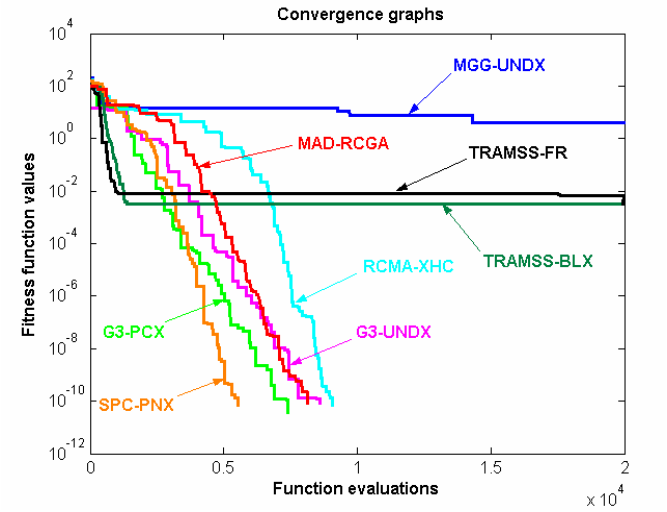


**Fig. 2.** Examples of typical convergence behavior of the algorithms on the neural model of an MD provided for ones of their best-performing runs.

| EA | Fitness function values | |
|---|---|---|
| | Best | Worst |
| **MGG-UNDX** | 3.9539e+000 | 3.2165e+01 |
| **G3-PCX** | $\leq 10^{-10}$ | 1.4242e+002 |
| **G3-UNDX** | $\leq 10^{-10}$ | 2.9348e+001 |
| **SPC-PNX** | $\leq 10^{-10}$ | **3.1431e+000** |
| **RCMA-XHC** | $\leq 10^{-10}$ | **3.1431e+000** |
| **TRAMSS-FR** | 1.1226e-005 | 2.1661e+001 |
| **TRAMSS-BLX** | 8.1813e-007 | 1.4242e+002 |
| **MAD-RCGA** | $\leq 10^{-10}$ | **3.1431e+000** |

**Tab. 2.** The best and worst values achieved by the algorithms on the MD model within 20 runs. The symbol $\leq 10^{-10}$ means that an algorithm succeeded in reaching the precision limit. The best results are printed bold.

## 4. The Design of Frequency-Selective Surfaces

In this section, the instances of the aforementioned algorithms will be applied to a numeric model of FSSs ([12], [15]). In brief, FSSs are periodic structures that consist of equidistantly distributed metallic elements placed on a dielectric substrate. At certain frequencies, FSSs behave like perfect conductors reflecting the bulk of the energy of incident electromagnetic waves. On the other hand, there are frequencies at which FSSs behave like dielectric layers having no metallic parts i.e., they transmit the bulk of the energy of incident waves.

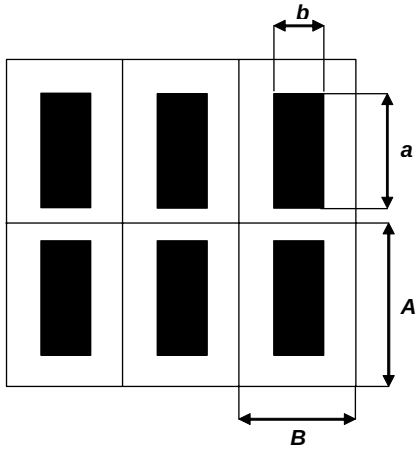


**Fig. 3.** Structure and parameters of the optimized FSS.

The numerical model has been developed by means of the Spectral-domain method of Moments [15] under the following assumptions:

- The metallic parts of the optimized FSS are made of perfect conductors.
- The conductive element is positioned in the center of a discrete cell of the infinite plane having the same electrical parameters as the surrounding environment.

The model was designed to have four input and one output parameters. The input parameters are as follows (Fig. 3):

- The height of a conductive element – $a$.
- The width of a conductive element – $b$.
- The height of a cell – $A$.
- The width of a cell – $B$.

The module of the reflection coefficient $\rho$ of the Floquet mode (0, 0) for an incident wave at frequency $f$ represents the output parameter of the model.

The objective of the optimization process is to search for such values of parameters $a$, $b$, $A$, $B$ of the FSS that maximize the module of $\rho$ (i.e., $|\rho| = 1$) for a frequency of 12 GHz so that its 3-dB decrease is observed at frequencies of 9 GHz and 15 GHz. The fitness function is defined as follows:

$$f_{fitness} = |\rho - 1|. \tag{2}$$

The optimization process is restricted to the following continuous search space:

- Allowed element heights are $a \in$ [0.5 mm; 20 mm].
- Allowed element widths are $b \in$ [0.5 mm; 3.0 mm].
- Allowed cell heights are $A \in$ [20 mm; 30 mm].
- Allowed cell widths are $B \in$ [3 mm; 10 mm].

### 4.1 Results

As stated in Section 1, the termination criterion regarding the maximum number of function evaluation was extended by another criterion prescribing a target accuracy of 0.1 so that if any of these two criteria is satisfied, the related run will be ended. This additional criterion is also used for estimating the computational reliability of the algorithms on this model (i.e., judged with respect to all the pre-defined restraints).

| EA | Fitness function evaluations | | | |
|---|---|---|---|---|
| | Best | Median | Worst | Success [%] |
| MGG-UNDX | 234 | 653 | 949 (0.198) | 65 |
| G3-PCX | 116 | 186 | 381 | 100 |
| G3-UNDX | 103 | 121 | 325 | 100 |
| SPC-PNX | 229 | 326 | 899 | 100 |
| RCMA-XHC | 619 | 788 | 935 (0.101) | 90 |
| TRAMSS-FR | 215 | 215 | 215 (0.289) | 5 |
| TRAMSS-BLX | - (0.205) | - | - (0.370) | 0 |
| MAD-RCGA | **78** | **98** | **167** | **100** |

**Tab. 3.** Performance comparisons carried out on the FSS model between the instances of the following algorithms: MGG-UNDX, G3-PCX, G3-UNDX, SPC-PNX, RCMA-XHC, TRAMSS-FR, TRAMSS-BLX and MAD-RCGA. The best, median and worst number of function evaluations needed for achieving a solution with a prescribed accuracy of 0.1 within a maximum number of $10^3$ evaluations. "Success" in the last column refers to how many runs reached the prescribed accuracy. Using a hyphen in cells means that an algorithm was not able to arrive at a solution with the prescribed accuracy in any run. The numbers in parentheses state the worst or best function values provided an algorithm was not able to arrive at a solution with the target accuracy in every run. The best results are printed bold.

The results that have been obtained by applying the algorithms to the numerical FSS model are tabulated in Tab. 3. When looking at the results summarized in Tab. 3, we can see that the best values, in terms of the performance metric used, are obtained by MAD-RCGA. Nonetheless, comparably good results were also obtained by G3-UNDX and, to some extent, by G3-PCX. The table also reveals that both of TRAMSS instances totally failed when trying to hit the precision limit within the maximum number of function evaluations. Nonetheless, the function values of both of the instances exhibited a descending tendency as the search advanced, so that if we increased the limit on the maximum number of function evaluations, the computational reliability of these instances would probably grow. In order to have some notion of their performances, the best and worst function values obtained over all their runs are stated in parentheses. A comparison of typical convergence behavior of the used algorithms made for their best-performing runs is depicted in Fig. 4. In the figure, none of graphs originates at the beginning of coordinates because of different population sizes used by the algorithms.

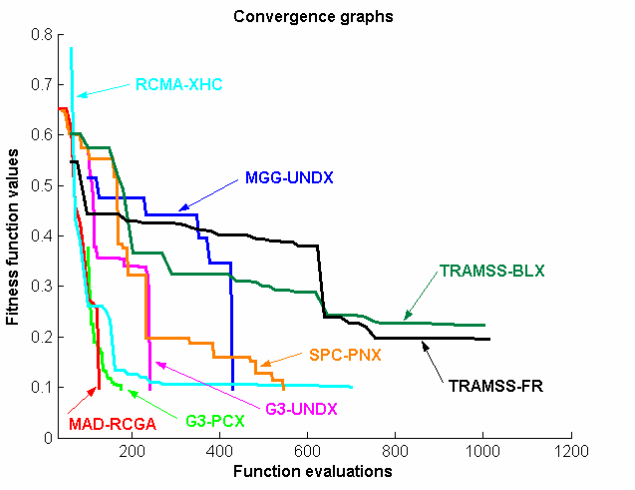


**Fig. 4.** Examples of typical convergence behavior of the algorithms on the FSS model provided for ones of their best-performing runs.

## 5. The Design of a Yagi Antenna

For the purpose of other tests of the RCGAs on real-life electromagnetic structures, a numerical model of a nine-part YA has been developed using the Method of Moments [3]. The model of the antenna was made under the following simplifying assumptions:

- The wires of the antenna are made of perfect conductors.
- The current flowing through the wires is concentrated along with the charge in the axes of the conductors.
- Each part of the antenna is split in segments of the same length. The reflector is by two segments longer than the active dipole (i.e., one per side) and each of the directors is by two segments smaller than the active dipole (i.e., one per side).

The parameters that have permission to vary during the optimization process are as follows (see Fig. 5):

- The length of the active dipole – $l$.
- The radius of the active dipole – $a$.
- Mutual distances between the wire parts of the antenna – $d_{ij}$ (i.e., it stands for distances between the particular antenna elements with subscripts having defined as depicted in Fig. 5).

The main goal of our optimization is to find such values of the parameters that minimize the input reactance $X$ of the antenna (i.e., to get closer to the resonance of the antenna). In the experiments, the antenna is supposed to be excited by a source having a wavelength of 0.68 meters. Minimi-

zing the input reactance of the antenna is accompanied by satisfying the following additional objectives:

- The gain $g$ of the antenna has to be equal to or higher than $g_0$ = 12 dB.
- The area of the surface of backward lobes $\eta$ has to be equal to or less than $\eta_0$ = 10 (i.e., it is a non-normalized value).

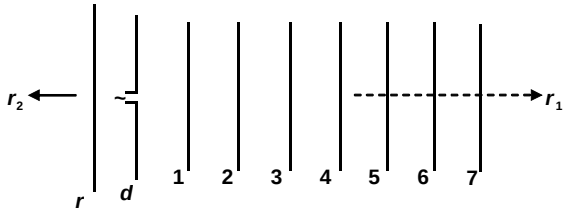


**Fig. 5.** Structure and parameters of the Yagi antenna.

Based on all the objectives of the optimization, the corresponding fitness function is defined by the following dimensionless form:

$$f_{fitness} = \sqrt{X^2 + w_1(g - g_0)^2 + w_2(\eta - \eta_0)^2} \qquad (3)$$

In (3), $w_1$ and $w_2$ are defined as follows. If ($g \geq g_0$) or ($\eta \leq \eta_0$), the corresponding symbol, i.e., $w_1$ or $w_2$, is switched to zero. Otherwise, it is set to one. The optimization process is permitted to vary the values of the parameters in the following continuous intervals:

- $l \in$ [0.2 m; 0.5 m]; $a \in$ [0.5 m; 1.5 m]$\cdot 10^{-3}$.
- $d_{rd} \in$ [0.2 m; 0.25 m]; $d_{d1} \in$ [0.2 m; 0.25 m].
- $d_{12} \in$ [0.27 m; 0.40 m]; $d_{23} \in$ [0.42 m; 0.55 m]; $d_{34} \in$ [0.57 m; 0.70 m].
- $d_{45} \in$ [0.72 m; 0.85 m]; $d_{56} \in$ [0.87 m; 1.00 m]; $d_{67} \in$ [1.02 m; 1.15 m].

## 5.1 Results

The results that have been obtained by applying the algorithms to the numerical model of the antenna are tabulated in Tab. 4. Here we can clearly see that the best result, in terms of the performance metric used, is achieved by the proposed algorithm. Nonetheless, the differences between three best-performing algorithms, i.e., MAD-RCGA, RCMA-XHC and SPC-PNX, are not significant. For demonstrational purposes, the best and worst values at which the algorithms arrived within the experiments are summarized in Tab. 5. Looking into the table, we can notice that the entirely best value was obtained by SPC-PNX. On the other hand, the best of the worst values was obtained by the proposed algorithm. The tables also show that the three best-performing algorithms produced the least spread of fitness function values over all their runs.

A comparison of typical convergence behavior of the used algorithms made for ones of their best-performing runs is depicted in Fig. 6. Moreover, an example of a radiation pattern belonging to the "E" plane and being obtained by MAD-RCGA after having completed $2\cdot 10^3$ function evaluations is given in Fig. 7. In this figure, the direction $r_1$ from Fig. 5 corresponds to an angle of 270°. This example is associated with a fitness value of 7.26 and the following values of output parameters $X$, $\eta$ and $g$:

- $|X|$ = 3.08 Ω,
- $\eta$ = 16.68,
- $g$ = 13.13 dB.

| EA | Fitness function values | |
|---|---|---|
| | Mean | Standard deviation |
| MGG-UNDX | 1.9787e+001 | 3.2797e+000 |
| G3-PCX | 1.6637e+001 | 5.1579e+000 |
| G3-UNDX | 1.4054e+001 | 5.8149e+000 |
| SPC-PNX | 9.0093e+000 | 1.4303e+000 |
| RCMA-XHC | 8.8998e+000 | 9.1235e-001 |
| TRAMSS-FR | 1.5538e+001 | 2.8152e+000 |
| TRAMSS-BLX | 1.6137e+001 | 3.8192e+000 |
| MAD-RCGA | **8.5203e+000** | **1.0761e+000** |

**Tab. 4.** The results of performance comparisons carried out on the YA model between the instances of the following algorithms: MGG-UNDX, G3-PCX, G3-UNDX, SPC-PNX, RCMA-XHC, TRAMSS-FR, TRAMSS-BLX and MAD-RCGA. The best results are printed bold.

| EA | Fitness function values | |
|---|---|---|
| | Best | Worst |
| MGG-UNDX | 1.3152e+001 | 2.6051e+001 |
| G3-PCX | 1.0091e+001 | 3.3341e+001 |
| G3-UNDX | 7.6690e+000 | 2.9545e+001 |
| SPC-PNX | **5.6218e+000** | 1.2277e+001 |
| RCMA-XHC | 7.5689e+000 | 1.1219e+001 |
| TRAMSS-FR | 1.0001e+001 | 2.1622e+001 |
| TRAMSS-BLX | 1.1157e+001 | 2.7232e+001 |
| MAD-RCGA | 7.2658e+000 | **1.0861e+001** |

**Tab. 5.** The best and worst values achieved by algorithms on the YA model within 20 runs. The best results printed bold.

# 6. Conclusions

The central story of the second part of this paper was applications of MAD-RCGA along with advanced and well-proved RCGA instances to problems in microwave technique, including their mutual comparison as regards the quality of achieved results. All the algorithms were applied to the design of an MD, the design of FSSs and the design of a YA. Except for the case of an MD where a neural model was used, all of the structures were represented by numerical models. As can clearly be seen by looking into the tables collecting the relevant data, all the RCGA instances were able to arrive at results of satisfactory quality under the predefined constraints. Nonetheless,

the instances of MAD-RCGA, RCMA-XHC and SPC-PNX were able to provide consistently-good results over the entire set of technical problems. Moreover, the proposed algorithmic solution, MAD-RCGA, outperformed the others on two of the three technical test problems with respect to the performance measures chosen.

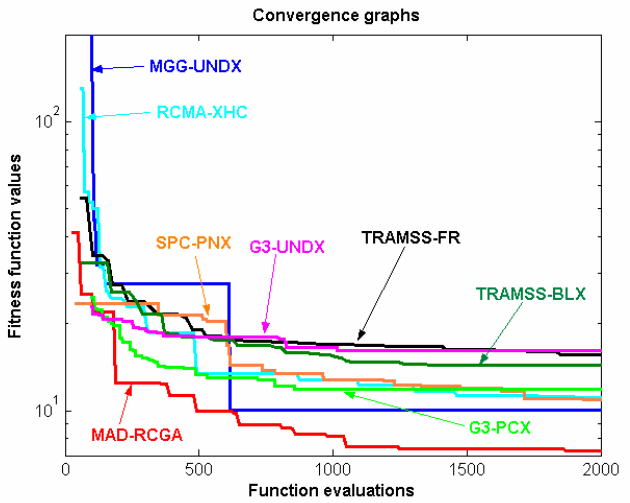


**Fig. 6.** Examples of typical convergence behavior of the algorithms on the YA model provided for ones of their best-performing runs.

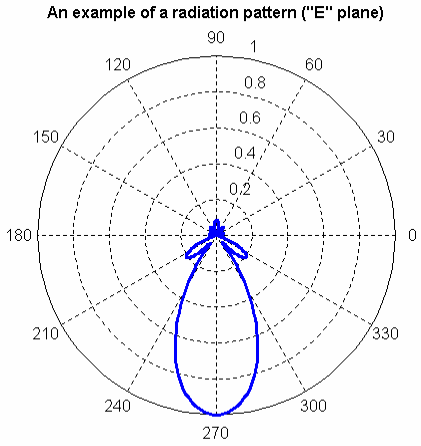


**Fig. 7.** An example of a radiation pattern obtained by MAD-RCGA for one of its typical runs on the YA model.

On the basis of the results achieved on the three technical "test" problems, we can conclude by saying that all of the presented algorithms have the real potential of being successfully applied to electromagnetic optimization. Moreover, the proposed algorithmic solution – MAD-RCGA – was able to provide ones of the best results, which is evidence of robustness of this algorithm.

## Acknowledgements

The research described in the paper was financially supported by the Czech Grant Agency under grant No. 102/07/0668, by the COST project IC0603 ASSIST, and by the research program MSM 0021630513.

## References

[1] BALLESTER, P. J., CARTER, J. N. An effective real-parameter genetic algorithm with parent centric normal crossover for multimodal optimization. In *Proc. of the Genetic and Evolutionary Computation Conference GECCO'04*. Springer-Verlag, 2004, p. 901-913.

[2] BEYER, H. G., DEB, K. On self-adaptive features in real-parameter evolutionary algorithms. *IEEE Tran. on Evolutionary Computation,* 2001, vol. 5, no. 3, p. 250–270.

[3] ČERNOHORSKÝ, D., RAIDA, Z., ŠKVOR, Z., NOVÁČEK, Z. *Analysis and Optimization of Microwave Structures*. Brno: VUTIUM Publishing, 1999. (In Czech).

[4] DEB, K., JOSHI, D., ANAND, A. *Real-Coded Evolutionary Algorithms with Parent-Centric Recombination.* KanGAL (Kanpur Genetic Algorithms Laboratory) Technical Report No. 2001003. Indian Institute of Technology Kanpur, 2001.

[5] DEB, K., ANAND, A., JOSHI, D. *A Computationally Efficient Evolutionary Algorithm for Real Parameter Optimization*. KanGAL (Kanpur Genetic Algorithms Laboratory) Technical Report No. 2002003. Indian Institute of Technology Kanpur, 2002.

[6] DEB, K., ANAND, A., JOSHI, D. A computationally efficient evolutionary algorithm for real parameter optimization. *Evolutionary Computation Journal*. MIT Press, 2002, vol. 10, no. 4, p. 371–395.

[7] DEB, K. *A Population-Based Algorithm Generator for Real Parameter Optimization.* KanGAL (Kanpur Genetic Algorithms Lab.) Technical Report No. 2003003. Indian Inst. of Techn. Kanpur, 2003.

[8] DEB, K. A population-based algorithm generator for real parameter optimization. *Soft Computing*. Springer-Verlag, 2005, vol. 9, no. 4, p. 236–253.

[9] HERRERA, F., LOZANO, M. Two-loop real-coded genetic algorithms with adaptive control of mutation step sizes. *Applied Intelligence*. Kluwer Academic Publishers, 2000, vol. 13, pp. 187–204.

[10] HERRERA, F., LOZANO, M., SÁNCHEZ, A. M. A taxonomy for the crossover operator for real-coded genetic algorithms: An experimental study. *International Journal of Intelligent Systems*. Wiley Periodicals, Inc., 2003, vol. 18, no. 3, p. 309–338.

[11] LOZANO, M., HERRERA, F., KRASNOGOR, N., MOLINA, D. Real-coded memetic algorithms with crossover hill-climbing. *Evolutionary Computation Journal.* MIT Press, 2004, vol. 12, p. 273–302.

[12] MUNK, B. A. *Frequency-Selective Surfaces: Theory and Design*. Chichester: J. Wiley & Sons, 2000.

[13] OTEVŘEL, V., RAIDA, Z. Wide band global optimization of microstrip line using novel polytope and real genetic algorithms. In *Proc. of the International Conference on Electromagnetics in Advanced Applications ICEAA'03*. Polytecnico di Torino, 2003, p. 131-134

[14] OTEVŘEL, V., RAIDA, Z. Mean-adaptive real-coding genetic algorithm and its application to electromagnetic optimization (part one). *Radioengineering*. 2007, vol. 16, no. 3, p. 19–29.

[15] SCOTT, C. *Spectral-Domain Method in Electromagnetics*. Norwood: Artech House, 1989.

## About Authors...

**Viktor OTEVŘEL** graduated at the Faculty of Electrical Engineering and Communication (FEEC), Brno University of Technology, in 2000. His main interests lie in the theory and applications of artificial intelligence, especially evolutionary algorithms.

**Zbyněk RAIDA –** for biography see p. 46 of this issue.